

Precision calculation of hyperfine structure of ${}^7,9\text{Be}^{2+}$ ions

Xiao-Qiu Qi^{1,2}, Pei-Pei Zhang^{2,4,†}, Zong-Chao Yan^{3,2}, Ting-Yun Shi², G. W. F. Drake⁴, Ai-Xi Chen¹, and Zhen-Xiang Zhong²

¹ Key Laboratory of Optical Field Manipulation of Zhejiang Province and Physics Department of Zhejiang Sci-Tech University, Hangzhou 310018, China

² State Key Laboratory of Magnetic Resonance and Atomic and Molecular Physics,

Wuhan Institute of Physics and Mathematics, Innovation Academy for Precision Measurement Science and Technology, Chinese Academy of Sciences, Wuhan 430071, China

³ Department of Physics, University of New Brunswick, Fredericton, New Brunswick, Canada E3B 5A3 and

⁴ Department of Physics, University of Windsor, Windsor, Ontario, Canada N9B 3P4

(Dated: March 11, 2022)

The hyperfine structures of the 2^3S_1 and 2^3P_J states of the ${}^7\text{Be}^{2+}$ and ${}^9\text{Be}^{2+}$ ions are investigated within the framework of the nonrelativistic quantum electrodynamics (NRQED). The uncertainties of present hyperfine splitting results of ${}^9\text{Be}^{2+}$ are in the order of several tens of ppm, where two orders of magnitude improvement over the previous theory and experiment values has been achieved. The contribution of nuclear electric quadrupole moment to hyperfine splitting of ${}^7\text{Be}^{2+}$ has been studied. A scheme for determining the properties of Be nuclei in terms of Zemach radius or the electric quadrupole moment based on precise spectra is proposed, and it opens a new window for the study of Be nuclei.

I. INTRODUCTION

Light helium and helium-like ions are among simplest atomic systems where theoretical approaches are well advanced to calculate their electronic structures with high precision. However, there are still unsolved interesting problems [1–7]. Among various theoretical methods, the nonrelativistic quantum electrodynamics (NRQED) is the most effective approach designed to calculate the electronic structure of light atomic systems [8–11]. For the helium 2^3P_J fine-structure, for example, the NRQED-based calculation has achieved a precision of about 1.7 kHz, far exceeding all other theoretical approaches that are based on Dirac-like methods [12]. Experimentally, Clausen *et al.* [13] have recently reported a much improved new determination of the He 2^1S ionization energy at the level of 32 kHz, which is in good accord with theory. However, the derived experimental ionization energies of the 2^3S and 2^3P states are in disagreement with theoretical prediction by 6.5σ and 10σ , respectively. Li^+ is very similar to helium with a higher Z , and its QED effect is more significant than helium. For the 2^3P_1 - 2^3P_2 fine structure interval for example, the contribution from order $m\alpha^6$ and higher in Li^+ is a factor of 26 larger than for helium [14]. The hyperfine structure splittings (hfs) of Li^+ have been studied in our previous work [5] using the NRQED theory. The theoretical uncertainty is reduced to be less than 100 kHz by a complete calculation of all the corrections up to $m\alpha^6$. The so-called Zemach radius, which describes the distribution of magnetic moment inside the nucleus, can be extracted by combining precision measurements [14]. The obtained Zemach ra-

dius for ${}^7\text{Li}$ is in good agreement with previous values, while the value for ${}^6\text{Li}$ disagrees with the nuclear physics value [15] by more than 6σ , indicating an anomalous nuclear structure for ${}^6\text{Li}$.

For further testing QED effect with low- Z ions, the helium-like Be^{2+} is a suitable candidates [16–18], since the transition wavelength of $2^3S - 2^3P$ of 372 nm is still close to the visible region. Beryllium has many isotopes ${}^6\text{Be}$ - ${}^{14}\text{Be}$ [19–22], including one-neutron halo ${}^{11}\text{Be}$ and two-neutron halo ${}^{14}\text{Be}$. There are some recent spectral experiments to explore Be nuclear structure [20, 22–24]. Puchalski *et al.* calculated the hyperfine splittings of ${}^9\text{Be}$ using explicitly correlated Gaussian function (ECG), and accurately determined the nuclear electric quadrupole moment [25], although it was inconsistent with the previous value. The advantage of studying Be^{2+} ion rather than neutral Be is that it is a three-body system for which the corresponding QED theory is relatively simpler. Compared with helium and Li^+ ions, the current research on Be^{2+} is rare. yanyan In 1993, Scholl *et al.* measured the $1s2s^3S_1 - 1s2p^3P_J$ transition of ${}^9\text{Be}^{2+}$ ion by applying fast ion beam laser fluorescence method with an accuracy of 10^{-8} [16], which is three orders of magnitude improvement over previous measurements. The fine and hyperfine splittings extracted are, respectively, in the order of tens of ppm and 10^{-4} . Theoretically, Johnson *et al.* in 1997 [26] calculated 2^3P_J hfs of ${}^9\text{Be}^{2+}$ by the relativistic configuration interaction method with only four significant digits. With the development of experimental technology, especially the emergence of new light sources of narrow linewidth in the XUV area [27–29], it is now possible to improve the measurement of Be^{2+} to reach a new

accuracy level.

In this paper, we intend to present a systematic calculation of hfs of the 2^3S_1 and 2^3P_J states of the $^{7,9}\text{Be}^{2+}$ ions by including QED corrections up to $m\alpha^6$ order. The possibility of determining the Zemach radius and the electric quadrupole moment of a Be isotope based on Be^{2+} spectroscopy is discussed. The present paper is organized as follows. Sec. II outlines the basic theoretical framework for our calculations. Sec. III details various QED contributions to the hfs of 2^3S_1 and 2^3P_J states of the $^{7,9}\text{Be}^{2+}$. Finally, discussions and conclusions are given in Sec. IV.

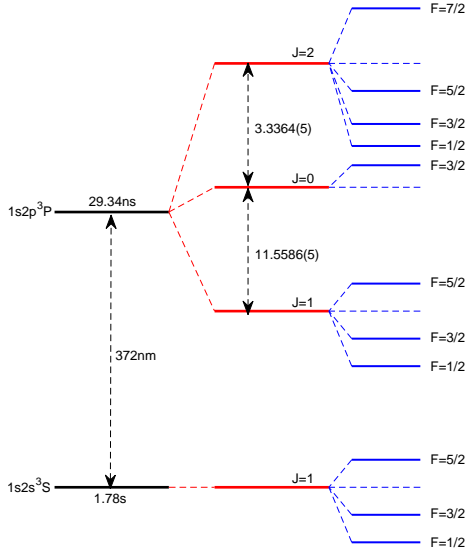


FIG. 1. Hyperfine energy levels (not drawn to scale) of the 2^3S_1 and 2^3P_J states of $^9\text{Be}^{2+}$ [16], in cm^{-1} . The nuclear spin of ^9Be is $3/2$.

II. THEORETICAL METHOD

The NRQED theory for quasidegenerate states is used to calculate fine and hyperfine structure splittings [4, 30–32]. The theory has been used in calculation of Li^+ hyperfine structure [5]. Here we simply outline the framework for calculating relativistic and QED corrections to an energy level. Figure 1 shows the energy level diagram of hfs for $^9\text{Be}^{2+}$ (The diagram for $^7\text{Be}^{2+}$ is similar to $^9\text{Be}^{2+}$ since they have the same nuclear spin $3/2$). In order to obtain the energies of the 2^3S_1 and 2^3P_J states, we need to diagonalize the effective Hamiltonian H with its matrix elements being

$$E_{JJ'}^F \equiv \langle JFM_F | H | J'FM_F \rangle, \quad (1)$$

where M_F is the projection of the total angular momentum F , which can be fixed arbitrarily since the energies

are independent of it. For convenience, we treat the 2^3P_J centroid as the zero level. The above matrix elements Eq. (1) can be expanded in powers of the fine structure constant α

$$\begin{aligned} E_{JJ'}^F = & \langle H_{\text{fs}} \rangle_J \delta_{JJ'} + \langle H_{\text{hfs}}^{(4+)} \rangle + \langle H_{\text{hfs}}^{(6)} \rangle \\ & + 2 \langle H_{\text{hfs}}^{(4)}, [H_{\text{nfs}}^{(4)} + H_{\text{fs}}^{(4)}] \rangle + \langle H_{\text{hfs}}^{(4)}, H_{\text{hfs}}^{(4)} \rangle \\ & + \langle H_{\text{QED}}^{(6)} \rangle + \langle H_{\text{QED}}^{\text{ho}} \rangle + \langle H_{\text{nucl}} \rangle + \langle H_{\text{eqm}} \rangle, \end{aligned} \quad (2)$$

where $\langle A, B \rangle \equiv \langle A \frac{1}{(E_0 - H_0)} B \rangle$, with H_0 and E_0 being the nonrelativistic Hamiltonian and its eigenvalue. H_{fs} is the effective operator that does not depend on the nuclear spin and is responsible for the fine structure splittings [12, 33]. The other terms in Eq. (2) are the nuclear spin dependent contributions. $H_{\text{hfs}}^{(4+)}$ is the leading-order hyperfine Hamiltonian of $m\alpha^4$, where the superscript ‘+’ means the higher-order terms from the recoil and anomalous magnetic moment effects. $H_{\text{hfs}}^{(6)}$ is the effective operator for the hyperfine splittings of order $m\alpha^6$. $H_{\text{fs}}^{(4)}$ and $H_{\text{nfs}}^{(4)}$ are the Breit Hamiltonians of order $m\alpha^4$ with and without electron spin. The fifth term in Eq. (2) is the second-order hyperfine correction, which contributes to the isotope shift, fine and hyperfine splittings. $H_{\text{QED}}^{(6)}$ and $H_{\text{QED}}^{\text{ho}}$ are the two effective operators for the QED corrections of order $m\alpha^6$ and higher $\sim m\alpha^7$. Finally, H_{nucl} and H_{eqm} represent the nuclear effects due to the Zemach radius and the nuclear electric quadrupole moment.

We solve the eigenvalue problem of H_0 variationally in Hylleraas coordinates. The relativistic and QED corrections as well as the corrections due to nuclear structure are evaluated perturbatively. The Hylleraas basis set [34] is constructed according to

$$\psi_{\ell m n}(\vec{r}_1, \vec{r}_2) = r_1^\ell r_2^m r^n e^{-\alpha r_1 - \beta r_2 - \gamma r} \mathcal{Y}_{\ell_1 \ell_2}^{LM}(\hat{r}_1, \hat{r}_2), \quad (3)$$

where $\vec{r} = \vec{r}_1 - \vec{r}_2$ and $\mathcal{Y}_{\ell_1 \ell_2}^{LM}(\hat{r}_1, \hat{r}_2)$ is the vector coupled product of spherical harmonics for the electrons. In order to deal with the nonrelativistic finite nuclear mass effect, according to whether the mass polarization operator is explicitly included in the nonrelativistic Hamiltonian, two different types of wave functions can be generated. For $\langle H_{\text{hfs}}^{(4+)} \rangle$, $\langle H_{\text{QED}}^{(6)} \rangle$, $\langle H_{\text{QED}}^{\text{ho}} \rangle$, $\langle H_{\text{nucl}} \rangle$, and $\langle H_{\text{eqm}} \rangle$, we use the wave functions with the mass polarization, whereas for other terms we use the wave functions corresponding to the infinite nuclear mass limit. The coupling of intermediate states of different symmetries should be included in the second-order terms, where some singular integrals need to be handled by including more singular terms in the intermediate states [35]. The necessary angular momentum operators, which can be evaluated analytically [5], are [31] $S^i L^i$, $I^i L^i$, $I^i S^i$, $\{S^i S^j\} \{L^i L^j\}$, $I^i S^j \{L^i L^j\}$,

$I^i L^j \{S^i S^j\}$, $\{I^i I^j\} \{S^i S^j\}$, $\{I^i I^j\} \{L^i L^j\}$, $\{I^i I^j\} L^i S^j$, and $\{I^i I^j\} \{S^m S^n\} \{L^k L^l\}^{ij}$, where $\{S^i S^j\} \equiv \frac{1}{2} S^i S^j + \frac{1}{2} S^j S^i - \frac{1}{3} \vec{S}^2 \delta^{ij}$ and the summation over the repeated indices is assumed.

III. THE HFS OF 2^3S_1 AND 2^3P_J STATES

The hfs operators responsible for relativistic and QED corrections to the 2^3S_1 and 2^3P_J states of helium-like ions are defined in our previous paper [5]. The first-order perturbation results of $m\alpha^4$ and $m\alpha^6$ corrections are listed in Table I.

TABLE I. Expectation values for the 2^3S_1 and 2^3P_J states of ${}^7\text{Be}^{2+}$ and ${}^9\text{Be}^{2+}$. The listed numerical values are uncertain only at the last digits. In atomic units.

State	Operator	${}^7\text{Be}^{2+}$	${}^9\text{Be}^{2+}$
2^3S_1	$4\pi\delta^3(\vec{r}_1)$	137.731960	137.739110
	K'	-157.232037	-157.232037
2^3P_J	$4\pi\delta^3(\vec{r}_1)$	126.232881	126.239606
	$(\vec{r}_1 \times \vec{p}_1)/r_1^3$	1.814143	1.814146
	$(\vec{r}_1 \times \vec{p}_2)/r_1^3$	-2.602150	-2.602181
	$(\delta^{ij} - 3r_1^i r_1^j / r_1^2)/r_1^3$	-0.671762	-0.671769
	K'	55.3670854	55.3670854
	\vec{K}	-145.86034	-145.86034
	\hat{K}	-82.07829	-82.07829

The second-order corrections of $m\alpha^6$ can be divided into several parts according to the symmetries of the intermediate states. For the 2^3S_1 state, the intermediate states are 3S , 3P , and 3D . And for 2^3P_J state the intermediate states are 3P , 1P , 3D , 1D , and 1F . Numerical results of various operators for the radial parts are presented in Table II. Since the second-order hyperfine correction $\langle H_{\text{hfs}}^{(4)}, H_{\text{hfs}}^{(4)} \rangle$ is divergent, we calculate only the dominant contribution from the 2^1P_1 intermediate state. It should be noted that the uncertainty of $\langle P_A, P_A \rangle^\circ$ in Table II is only computational. We also use the method in Ref. [31] to estimate the uncertainty due to this approximation, *i.e.*, calculating the second-order perturbation for the operator $\langle P'_A, P'_A \rangle$, and taking the difference between $\langle P_A, P_A \rangle^\circ$ and $\langle P'_A, P'_A \rangle$ as the uncertainty, which is 10000 a.u. for 2^3S_1 and 15000 a.u. for 2^3P_J respectively.

We calculate the hfs of the 2^3S_1 and 2^3P_J states using the values in Tables I and II. Since the contribution from the $1s$ electron dominates higher-order QED correction, the assumption that $H_{\text{QED}}^{\text{ho}}(1s2p) \simeq H_{\text{QED}}^{\text{ho}}(1s)$ is adopted for the hfs calculation of the 2^3P_J state, while the $H_{\text{QED}}^{\text{ho}}(1s2s)$ of 2^3S_1 state is approximated by the weighted average of $H_{\text{QED}}^{\text{ho}}(1s)$ and $H_{\text{QED}}^{\text{ho}}(2s)$. The uncertainty of the correction $H_{\text{QED}}^{\text{ho}}$ is estimated as 20%

TABLE II. Second-order matrix elements for all possible intermediate states connected to the 2^3S_1 and 2^3P_J states. The listed numerical values are uncertain only at the last digits when not given explicitly. In atomic units.

State	Symmetry	$\langle A, B \rangle$	Value	
2^3S_1	3S	$\langle P', \vec{G}' \rangle$	4592.8	
	3P	$\langle \vec{P}, \vec{G} \rangle$	0.140	
	3D	$\langle \hat{P}, \vec{G} \rangle$	0.87	
	1S	$\langle P_A, P_A \rangle^\circ$	-839249.282	
2^3P_J	3P	$\langle P'_A, P'_A \rangle$	-848800(200)	
		$\langle P', \vec{G}' \rangle$	4024.6(5)	
	3D	$\langle \vec{P}, \vec{G} \rangle$	86.9(5)	
		$\langle \hat{P}, \vec{G} \rangle$	40(5)	
		$\langle P, \vec{G} \rangle$	26.678	
		$\langle \vec{P}, \vec{G} \rangle$	-64.1	
		$\langle \hat{P}, \vec{G} \rangle$	-39.8427	
		$\langle P, \vec{G} \rangle$	6.714(5)	
		$\langle \vec{P}, \vec{G} \rangle$	19.323	
		$\langle \hat{P}, \vec{G} \rangle$	8.882	
		1P	$\langle P_A, \vec{G}_A \rangle$	9054.88(5)
			$\langle P_A, \vec{G}_A \rangle^\circ$	9021.158
		3D	$\langle \hat{P}_A, \vec{G}_A \rangle$	-176.7(5)
			$\langle \hat{P}_A, \vec{G}_A \rangle^\circ$	-139.044
$\langle \vec{P}, \vec{G} \rangle$	0.044			
$\langle \hat{P}, \vec{G} \rangle$	-0.0149824			
$\langle \vec{P}, \vec{G} \rangle$	1.563(5)			
$\langle \hat{P}, \vec{G} \rangle$	-0.0688			
1D	$\langle \hat{P}_A, \vec{G}_A \rangle$		0.348(5)	
3F	$\langle \hat{P}, \vec{G} \rangle$		0.628(5)	
1P	$\langle P_A, P_A \rangle^\circ$	-1785103.485		
	$\langle P'_A, P'_A \rangle$	-1797300(200)		
	$\langle P_A, \hat{P}_A \rangle^\circ$	27527.773		
	$\langle \hat{P}_A, \hat{P}_A \rangle^\circ$	-2547.006		

of its contribution. According to Eq. (2), the hfs calculation of the 2^3P_J state requires the results of the fine structure splittings, which are $\langle H_{fs} \rangle_{J=0} = (8f_{01} + 5f_{12})/9$, $\langle H_{fs} \rangle_{J=1} = (-f_{01} + 5f_{12})/9$, and $\langle H_{fs} \rangle_{J=2} = (-f_{01} - 4f_{12})/9$, relative to the 2^3P_J centroid, with $f_{01} = 11.5586(5) \text{ cm}^{-1}$ and $f_{12} = -14.8950(4) \text{ cm}^{-1}$ for ${}^9\text{Be}^{2+}$ [16]. The fine structure splittings of ${}^7\text{Be}^{2+}$ are obtained by changing the reduced mass accordingly *i.e.*, $f_{01} = 11.558(2) \text{ cm}^{-1}$ and $f_{12} = -14.895(2) \text{ cm}^{-1}$. For ${}^7\text{Be}^{2+}$ and ${}^9\text{Be}^{2+}$, the magnetic moments are $-1.39928(2) \mu_N$ [36] and $-1.177432(3) \mu_N$ [20], and the nuclear electric quadrupole moments -6.11 fm^2 (the theoretical result from [37]) and $5.350(14) \text{ fm}^2$ [25], respectively. The contributions of Zemach radii are at $-615(8) \text{ ppm}$ [25] for ${}^9\text{Be}^{2+}$ and $-521(16) \text{ ppm}$ for ${}^7\text{Be}^{2+}$. This contribution of ${}^7\text{Be}^{2+}$ is calculated by $-2ZR_{\text{em}}/a_0$, where $R_{\text{em}} = 4R_e/\sqrt{3\pi}$ (Gaussian distributions) and the nuclear charge radius R_e is $2.647(17) \text{ fm}$ [20]. The hfs of 2^3S_1 and 2^3P_J states can be ob-

tained by diagonalizing the matrix in Eq. (2) and the results relative to the 2^3S_1 and 2^3P_J centroids are listed in Table III.

TABLE III. Theoretical results for individual $2^3S_1^F$ and $2^3P_J^F$ levels in ${}^7\text{Be}^{2+}$ and ${}^9\text{Be}^{2+}$, relative to the 2^3S_1 and 2^3P_J centroid respectively, where the first error in 2^3P state is due to the fine structure and the second error is due to the hyperfine structure, in cm^{-1} .

State	(J, F)	${}^7\text{Be}^{2+}$	${}^9\text{Be}^{2+}$
2^3S	(1, 1/2)	0.68251(1)	0.574282(6)
	(1, 3/2)	0.27300(1)	0.229708(3)
	(1, 5/2)	-0.40950(1)	-0.344566(4)
2^3P	(2, 1/2)	5.90767(100)(1)	5.817172(190)(4)
	(2, 3/2)	5.72041(100)(1)	5.658805(190)(3)
	(2, 5/2)	5.40467(100)(1)	5.392683(190)(1)
	(2, 7/2)	4.95513(100)(1)	5.015548(190)(3)
	(0, 3/2)	2.01174(200)(1)	2.008479(500)(1)
	(1, 1/2)	-9.23556(110)(1)	-9.287087(230)(3)
	(1, 3/2)	-9.44648(110)(1)	-9.461891(230)(1)
	(1, 5/2)	-9.75933(110)(1)	-9.727037(230)(2)

For the 2^3P_J states, the $2^1P_1 - 2^3P_1$ mixing effect should be taken into consideration carefully. Here we follow two methods used in our previous calculation [5]. Method 1. Do an exact diagonalization only within the 2^3P_J manifold and treat the $2^1P_1 - 2^3P_1$ mixing effect by perturbation theory up to second order. Method 2. Extend the 2^3P_J manifold by including the 2^1P_1 state and do an exact diagonalization of the extended matrix. Both the methods only include the relativistic correction of order $m\alpha^4$. The second-order matrix elements involving the intermediate state 2^1P_1 and the hyperfine structure coefficients [33] for the 2^1P_1 and 2^3P_J states are listed in Tables II and IV, as inputs for applying Methods 1 and 2. The hfs of 2^3P_J are evaluated using these two methods and the results are presented in Table V. The modification of the mixing effect alters the hyperfine intervals $(1, 1/2) - (1, 3/2)$ and $(1, 3/2) - (1, 5/2)$ by 0.000322 cm^{-1} and 0.000516 cm^{-1} for ${}^9\text{Be}^{2+}$, whereas for ${}^7\text{Be}^{2+}$ they are 0.00038 cm^{-1} and 0.00061 cm^{-1} , respectively. These shifts are about three orders of magnitude larger than that of ${}^7\text{Li}^+$. Our final results of 2^3P_J hfs for ${}^7\text{Be}^{2+}$ and ${}^9\text{Be}^{2+}$ are shown in Tables VI and Table VII.

IV. DISCUSSION AND CONCLUSION

The radioactive ${}^7\text{Be}$ is a special atomic nucleus whose magnetic moment cannot be obtained by the $\beta\gamma$ -NMR method, and optical spectroscopy is the only method to measure the nuclear moment. Although Okada *et al.* [36] determined the magnetic dipole moment of ${}^7\text{Be}$ to high accuracy, its charge radius has not been determined until now. In addition, there is no published value for the nuclear electric quadrupole moment of ${}^7\text{Be}$. For-

TABLE IV. Calculated values of ${}^7\text{Be}^{2+}$ and ${}^9\text{Be}^{2+}$ hfs coefficients for the 2^1P_1 and 2^3P_J states, in cm^{-1} . These coefficients are defined in Eqs. (10)-(12) of Ref. [33]. The listed numerical values are uncertain only at the last digits.

Coefficient	${}^7\text{Be}^{2+}$	${}^9\text{Be}^{2+}$
$C_{1,1}^{(0)}$	-0.24990	-0.210283
$C_{1,0}^{(0)}$	-0.25126	-0.211428
$D_1^{(0)}$	-0.00440	-0.003701
$D_0^{(0)}$	-0.00317	-0.002663
$E_{1,1}^{(0)}$	0.00112	0.000938
$E_{1,0}^{(0)}$	0.00097	0.000815

TABLE V. Hyperfine splittings in 2^3P_J of ${}^7\text{Be}^{2+}$ and ${}^9\text{Be}^{2+}$, in cm^{-1} . Only the relativistic correction of order $m\alpha^4$ is included. The listed numerical values are uncertain only at the last digits.

	$(J, F) - (J', F')$	Method 1	Method 2	Difference
${}^7\text{Be}^{2+}$	(2, 1/2) - (2, 3/2)	0.18729	0.18729	
	(2, 3/2) - (2, 5/2)	0.31552	0.31552	
	(2, 5/2) - (2, 7/2)	0.44873	0.44872	-0.00001
	(1, 1/2) - (1, 3/2)	0.21031	0.21069	0.00038
	(1, 3/2) - (1, 5/2)	0.31267	0.31328	0.00061
${}^9\text{Be}^{2+}$	(2, 1/2) - (2, 3/2)	0.157960	0.157964	0.000004
	(2, 3/2) - (2, 5/2)	0.265658	0.265660	0.000002
	(2, 5/2) - (2, 7/2)	0.376899	0.376891	-0.000008
	(1, 1/2) - (1, 3/2)	0.174864	0.175186	0.000322
	(1, 3/2) - (1, 5/2)	0.264669	0.265185	0.000516

tunately, although ${}^7\text{Be}$ is not stable, its half-life is about 53 days, which is helpful for the experimental measurement of ${}^7\text{Be}$. Since the quadrupole moment Q_d of ${}^7\text{Be}$ has not been measured and the results obtained by theoretical calculations differ noticeably from each other (-6.11 fm^2 [37], $-5.50(48) \text{ fm}^2$ and $-4.68(28) \text{ fm}^2$ [38]), these values are not yet conclusive. Here we study the contribution of the quadrupole moment Q_d to hfs of ${}^7\text{Be}^{2+}$ by ignoring its higher-order nonlinear correction,

$$E_d = E_a + Q_d(X + \delta X), \quad (4)$$

where E_d and E_a represent the hfs obtained by diagonalization of Eq. (2) with and without the contribution of Q_d ($\langle H_{\text{eqm}} \rangle$ term). X and δX are two linear coefficients independent of Q_d , where X is obtained from the diagonal element of the $\langle H_{\text{eqm}} \rangle$ term, and δX comes from the linear correction caused by the $\langle H_{\text{eqm}} \rangle$ term included in the diagonalization process. In order to reflect the sensitivity of the transitions to Q_d intuitively, one can define the relative accuracy,

$$\eta = \left| \frac{Q_d(X + \delta X)}{E_d} \right|. \quad (5)$$

TABLE VI. Theoretical hyperfine intervals in the 2^3S_1 and 2^3P_J states of ${}^7\text{Be}^{2+}$ with quadrupole moment $Q_d = -6.11 \text{ fm}^2$. The listed numerical values are uncertain only at the last digits.

State	$(J, F) - (J', F')$	E_a cm^{-1}	$10^5 X$ $\text{cm}^{-1}/\text{fm}^2$	$10^6 \delta X$ $\text{cm}^{-1}/\text{fm}^2$	η ppm	E_d cm^{-1}
2^3P_2	$(2, 1/2) - (2, 3/2)$	0.18751	4.12051	0.30	1354	0.18726
	$(2, 3/2) - (2, 5/2)$	0.31591	2.94322	-2.04	530	0.31574
	$(2, 5/2) - (2, 7/2)$	0.44928	-4.12051	1.02	546	0.44953
2^3P_1	$(1, 1/2) - (1, 3/2)$	0.21097	-5.29780	-0.43	1544	0.21130
	$(1, 3/2) - (1, 5/2)$	0.31365	2.94322	2.17	616	0.31346
2^3S_1	$(1, 1/2) - (1, 3/2)$	0.40951				0.40951
	$(1, 3/2) - (1, 5/2)$	0.68250				0.68250

TABLE VII. Experimental and theoretical hyperfine intervals in the 2^3S_1 and 2^3P_J states of ${}^9\text{Be}^{2+}$, in cm^{-1} .

State	$(J, F) - (J', F')$	Experiment		Theory	
		Scholl <i>et al.</i> [16]	Johnson <i>et al.</i> [26]	This work	
2^3P_2	$(2, 1/2) - (2, 3/2)$	0.1585(10)	0.1581	0.158371(7)	
	$(2, 3/2) - (2, 5/2)$	0.2659(11)	0.2659	0.266123(4)	
	$(2, 5/2) - (2, 7/2)$	0.3768(14)	0.3773	0.377128(4)	
2^3P_1	$(1, 1/2) - (1, 3/2)$	0.1751(10)	0.1754	0.175126(4)	
	$(1, 3/2) - (1, 5/2)$	0.2654(10)	0.2654	0.265662(3)	
2^3S_1	$(1, 1/2) - (1, 3/2)$	0.3448(10)		0.344574(9)	
	$(1, 3/2) - (1, 5/2)$	0.5740(11)		0.574275(6)	

In other words, the η is the precision required to detect the contribution of Q_d in the experiment. Using the theoretical value $Q_d = -6.11 \text{ fm}^2$ chosen in the Ref. [30], we calculated the results as shown in Table VI. The results show that the transitions $(1, 1/2) - (1, 3/2)$ and $(2, 1/2) - (2, 3/2)$ are more suitable to be used to determine the Q_d . According to the theoretical values, the value of Q_d is likely to exist between -7 fm^2 and -4 fm^2 . In this range, once the experiment reaches the same accuracy as the theory, the result of the Q_d can be determined according to the Eq. (5), and the accuracy can have two significant digits.

Table VII lists the experimental and theoretical hyperfine intervals in the 2^3P_J state of ${}^9\text{Be}^{2+}$, where the uncertainties are mainly due to the $m\alpha^7$ contribution and the nuclear structure. It is worth noting that these theoretical uncertainties are propagated only from the errors displayed in Table III. The uncertainty from the fine structure is canceled for the same- J transitions. Table VII also shows the measured results obtained through weighted average of all the values in Ref. [16], and the only available theoretical values of Johnson *et al.* [26] for the 2^3P_J state. Our results are in good agreement with these previous values and are about two orders of magnitude more precise. Our theoretical calculation has reached the level of ten or so ppm, which is sensitive to some of the major nuclear electromagnetic structure effect.

In summary, we have studied the hfs of the 2^3S_1 and 2^3P_J states of the ${}^7\text{Be}^{2+}$ and ${}^9\text{Be}^{2+}$ ions, including the

relativistic and QED corrections up to order $m\alpha^6$. The $2^1P_1 - 2^3P_1$ single-triple mixing effect has been treated rigorously. Compared to Li^+ , the $2^1P_1 - 2^3P_1$ mixing effect is about three orders of magnitude larger, indicating that this procedure becomes more and more essential with increasing Z . The uncertainties of present calculations are in the order of tens of ppm for ${}^9\text{Be}^{2+}$, mainly from the error of $m\alpha^7$ and nuclear contribution (the Zemach radius). The results for the hfs of the 2^3S_1 and 2^3P_J states have been improved by two orders of magnitude. The contribution of nuclear electric quadrupole moment to the hyperfine splittings of ${}^7\text{Be}^{2+}$ has also been studied. In order to observe the influence of Q_d , the precision of experimental measurements on hfs needs to be better than 10^{-4} cm^{-1} . If the experiments reach the same accuracy as the present theoretical value, the two significant digits of Q_d can be determined. Our results may stimulate further experimental activities to explore Be nuclear structure.

†Email address: zhangpei@wipm.ac.cn

- [1] Z.-C. Yan and G. W. F. Drake, High precision calculation of fine structure splittings in helium and He-like ions, *Phys. Rev. Lett.* **74**, 4791 (1995).
- [2] V. c. v. Patkóš, V. A. Yerokhin, and K. Pachucki, Higher-order recoil corrections for triplet states of the helium atom, *Phys. Rev. A* **94**, 052508 (2016).
- [3] V. c. v. Patkóš, V. A. Yerokhin, and K. Pachucki, Higher-order recoil corrections for singlet states of the helium atom, *Phys. Rev. A* **95**, 012508 (2017).
- [4] V. c. v. Patkóš, V. A. Yerokhin, and K. Pachucki, Complete quantum electrodynamic $\alpha^6 m$ correction to energy levels of light atoms, *Phys. Rev. A* **100**, 042510 (2019).
- [5] X.-Q. Qi, P.-P. Zhang, Z.-C. Yan, G. W. F. Drake, Z.-X. Zhong, T.-Y. Shi, S.-L. Chen, Y. Huang, H. Guan, and K.-L. Gao, Precision calculation of hyperfine structure and the zemach radii of ${}^{6,7}\text{Li}^+$ ions, *Phys. Rev. Lett.* **125**, 183002 (2020).
- [6] V. c. v. Patkóš, V. A. Yerokhin, and K. Pachucki, Complete $\alpha^7 m$ lamb shift of helium triplet states, *Phys. Rev. A* **103**, 042809 (2021).
- [7] V. c. v. Patkóš, V. A. Yerokhin, and K. Pachucki, Ra-

- diative $\alpha^7 m$ QED contribution to the helium lamb shift, *Phys. Rev. A* **103**, 012803 (2021).
- [8] K. Pachucki, U. D. Jentschura, and V. A. Yerokhin, Nonrelativistic QED approach to the bound-electron g factor, *Phys. Rev. Lett.* **93**, 150401 (2004).
- [9] K. Pachucki, U. D. Jentschura, and V. A. Yerokhin, Erratum: Nonrelativistic QED approach to the bound-electron g factor [phys. rev. lett. 93, 150401 (2004)], *Phys. Rev. Lett.* **94**, 229902 (2005).
- [10] U. D. Jentschura, A. Czarnecki, and K. Pachucki, Nonrelativistic QED approach to the lamb shift, *Phys. Rev. A* **72**, 062102 (2005).
- [11] K. Pachucki, V. c. v. Patkóš, and V. A. Yerokhin, Testing fundamental interactions on the helium atom, *Phys. Rev. A* **95**, 062510 (2017).
- [12] K. Pachucki and V. A. Yerokhin, Fine structure of heliumlike ions and determination of the fine structure constant, *Phys. Rev. Lett.* **104**, 070403 (2010).
- [13] G. Clausen, P. Jansen, S. Scheidegger, J. A. Agner, H. Schmutz, and F. Merkt, Ionization energy of the metastable 2^1S_0 state of ^4He from rydberg-series extrapolation, *Phys. Rev. Lett.* **127**, 093001 (2021).
- [14] H. Guan, S. Chen, X.-Q. Qi, S. Liang, W. Sun, P. Zhou, Y. Huang, P.-P. Zhang, Z.-X. Zhong, Z.-C. Yan, G. W. F. Drake, T.-Y. Shi, and K. Gao, Probing atomic and nuclear properties with precision spectroscopy of fine and hyperfine structures in the $^7\text{Li}^+$ ion, *Phys. Rev. A* **102**, 030801(R) (2020).
- [15] V. A. Yerokhin, Hyperfine structure of Li and Be^+ , *Phys. Rev. A* **78**, 012513 (2008).
- [16] T. J. Scholl, R. Cameron, S. D. Rosner, L. Zhang, R. A. Holt, C. J. Sansonetti, and J. D. Gillaspay, Precision measurement of relativistic and QED effects in heliumlike beryllium, *Phys. Rev. Lett.* **71**, 2188 (1993).
- [17] Z.-C. Yan, W. Nörtershäuser, and G. W. F. Drake, High precision atomic theory for Li and Be^+ : QED shifts and isotope shifts, *Phys. Rev. Lett.* **100**, 243002 (2008).
- [18] W. Nörtershäuser, C. Geppert, A. Krieger, K. Pachucki, M. Puchalski, K. Blaum, M. L. Bissell, N. Frömmgen, M. Hammen, M. Kowalska, J. Krämer, K. Kreim, R. Neugart, G. Neyens, R. Sánchez, and D. T. Jordanov, Precision test of many-body QED in the Be^+ $2P$ fine structure doublet using short-lived isotopes, *Phys. Rev. Lett.* **115**, 033002 (2015).
- [19] M. Labiche, F. M. Marqués, O. Sorlin, and N. Vinh Mau, Structure of ^{13}Be and ^{14}Be , *Phys. Rev. C* **60**, 027303 (1999).
- [20] W. Nörtershäuser, D. Tiedemann, M. Žáková, Z. Andjelkovic, K. Blaum, M. L. Bissell, R. Cazan, G. W. F. Drake, C. Geppert, M. Kowalska, J. Krämer, A. Krieger, R. Neugart, R. Sánchez, F. Schmidt-Kaler, Z.-C. Yan, D. T. Jordanov, and C. Zimmermann, Nuclear charge radii of $^{7,9,10}\text{Be}$ and the one-neutron halo nucleus ^{11}Be , *Phys. Rev. Lett.* **102**, 062503 (2009).
- [21] H. T. Fortune and R. Sherr, Consistent description of ^{11}Be and ^{12}Be and of the $^{11}\text{Be}(d,p)^{12}\text{Be}$ reaction, *Phys. Rev. C* **85**, 051303 (2012).
- [22] A. Krieger, K. Blaum, M. L. Bissell, N. Frömmgen, C. Geppert, M. Hammen, K. Kreim, M. Kowalska, J. Krämer, T. Neff, R. Neugart, G. Neyens, W. Nörtershäuser, C. Novotny, R. Sánchez, and D. T. Jordanov, Nuclear charge radius of ^{12}Be , *Phys. Rev. Lett.* **108**, 142501 (2012).
- [23] Z.-T. Lu, P. Mueller, G. W. F. Drake, W. Nörtershäuser, S. C. Pieper, and Z.-C. Yan, Colloquium: Laser probing of neutron-rich nuclei in light atoms, *Rev. Mod. Phys.* **85**, 1383 (2013).
- [24] W. Nörtershäuser, C. Geppert, A. Krieger, K. Pachucki, M. Puchalski, K. Blaum, M. L. Bissell, N. Frömmgen, M. Hammen, M. Kowalska, J. Krämer, K. Kreim, R. Neugart, G. Neyens, R. Sánchez, and D. T. Jordanov, Precision test of many-body QED in the Be^+ $2P$ fine structure doublet using short-lived isotopes, *Phys. Rev. Lett.* **115**, 033002 (2015).
- [25] M. Puchalski, J. Komasa, and K. Pachucki, Hyperfine structure of the 2^3P state in ^9Be and the nuclear quadrupole moment, *Phys. Rev. Research* **3**, 013293 (2021).
- [26] W. R. Johnson, K. T. Cheng, and D. R. Plante, Hyperfine structure of 2^3P levels of heliumlike ions, *Phys. Rev. A* **55**, 2728 (1997).
- [27] R. J. Jones, K. D. Moll, M. J. Thorpe, and J. Ye, Phase-coherent frequency combs in the vacuum ultraviolet via high-harmonic generation inside a femtosecond enhancement cavity, *Phys. Rev. Lett.* **94**, 193201 (2005).
- [28] A. Cingöz, D. C. Yost, T. K. Allison, A. Ruehl, M. E. Fermann, I. Hartl, and J. Ye, Direct frequency comb spectroscopy in the extreme ultraviolet, *Nature* **482**, 68 (2012).
- [29] J. Zhang, L.-Q. Hua, Z. Chen, M.-F. Zhu, C. Gong, and X.-J. Liu, Extreme ultraviolet frequency comb with more than 100 μw average power below 100nm, *Chin. Phys. Lett.* **37**, 124203 (2020).
- [30] M. Puchalski and K. Pachucki, Fine and hyperfine splitting of the $2P$ state in Li and Be^+ , *Phys. Rev. A* **79**, 032510 (2009).
- [31] K. Pachucki, V. A. Yerokhin, and P. Cancio Pastor, Quantum electrodynamic calculation of the hyperfine structure of ^3He , *Phys. Rev. A* **85**, 042517 (2012).
- [32] M. Haidar, Z.-X. Zhong, V. I. Korobov, and J.-P. Karr, Nonrelativistic QED approach to the fine- and hyperfine-structure corrections of order $m\alpha^6$ and $m\alpha^6(m/m)$: Application to the hydrogen atom, *Phys. Rev. A* **101**, 022501 (2020).
- [33] E. Riis, A. G. Sinclair, O. Poulsen, G. W. F. Drake, W. R. C. Rowley, and A. P. Levick, Lamb shifts and hyperfine structure in $^6\text{Li}^+$ and $^7\text{Li}^+$: Theory and experiment, *Phys. Rev. A* **49**, 207 (1994).
- [34] P.-P. Zhang, Z.-X. Zhong, Z.-C. Yan, and T.-Y. Shi, Precision calculation of fine structure in helium and Li^+ , *Chin. Phys. B* **24**, 033101 (2015).
- [35] G. W. F. Drake, Progress in helium fine-structure calculations and the fine-structure constant, *Can. J. Phys.* **80**, 1195 (2002).
- [36] K. Okada, M. Wada, T. Nakamura, A. Takamine, V. Lioubimov, P. Schury, Y. Ishida, T. Sonoda, M. Ogawa, Y. Yamazaki, Y. Kanai, T. M. Kojima, A. Yoshida, T. Kubo, I. Katayama, S. Ohtani, H. Wollnik, and H. A. Schuessler, Precision measurement of the hyperfine structure of laser-cooled radioactive $^7\text{Be}^+$ ions produced by projectile fragmentation, *Phys. Rev. Lett.* **101**, 212502 (2008).
- [37] A. Koji, O. Yoko, S. Yasuyuki, and V. Kálmán, Microscopic multicluster description of light exotic nuclei

- with stochastic variational method on correlated gaussians, [Prog. Theor. Phys. Suppl. **142**, 97 \(2001\)](#).
- [38] C. Forssén, E. Caurier, and P. Navrátil, Charge radii and electromagnetic moments of Li and Be isotopes from the ab initio no-core shell model, [Phys. Rev. C **79**, 021303 \(2009\)](#).